Chitosan-functionalized porous silicon optical transducer for the detection of carboxylic acid-containing drugs in water

Beniamino Sciacca,[ab] Emilie Secret,[a] Stéphanie Pace,[a] Philippe Gonzalez,[a] Francesco Geobaldo,[b] Françoise Quignard[a] and Frédérique Cunin*[a]

A chitosan/porous silicon biosensing platform for the detection of carboxylic acid-containing drugs in water is prepared and characterized. Parasitic layer-free films of mesoporous silicon are electrochemically etched and functionalized by covalent attachment of chitosan oligomers. The presence of the chitosan species covering the inner and outer surface of the porous silicon films is confirmed by infrared spectroscopy and nitrogen adsorption analysis. The obtained hybrid platform offers both an important porosity, with a higher surface area than the original porous silicon substrate, and an important surface charge, very suitable for sensing charged molecules. Ibuprofen is chosen as a drug model for the sensing experiments in water. Optical interferometry measurements are performed on the chitosan/porous silicon substrate exposed to ibuprofen solutions of various concentrations, and compared to the same experiments performed on a nonfunctionalized porous silicon surface. Results of the sensing experiments show that the presence of chitosan increases the sensitivity of the sensing porous film by more than one order of magnitude compared to the nonfunctionalized porous film. Detection in water of BHB, a model molecule for illicit rape drug GHB, is also demonstrated at concentrations compatible with forensic analysis, using the chitosan/porous silicon hybrid platform.

Introduction

The development of sensors for the detection of specific organic compounds dissolved in water is of major interest for the preservation of aquatic environment and water quality, in the biomedical field for immunodiagnostic and toxicology studies, and in forensic medicine for the detection and identification of illicit drugs. Analytical techniques of choice currently used for determining the presence of organic chemicals and drugs in water include gas chromatography/mass spectrometry, liquid chromatography/tandem mass spectrometry, and capillary electrophoresis.[1–3] However the development of portable analytical instruments that combine sensitivity and selectivity, and a minimal consumption of sample per analysis is still a challenge. Innovative sensing approaches are based on nanotechnology by the development of lab-on-chip-like systems which incorporate affinity-based chemical or biological recognition (ligand/receptor, antigen/antibody, DNA/DNA, supramolecular chemistry, *etc.*) and a transducer mode (electrochemical, optical, *etc.*).[4–8]

Porous silicon (pSi) is a material obtained from an electrochemical etch of crystalline silicon which conjugates tunable structural and optical properties. Due to its great potential to be functionalized *via* surface chemistry, pSi has proved efficient as a platform for the development of optical label free chemo and biosensors.[9–20] Indeed surface chemistry provides a means to specifically functionalize the sensing substrate in order to detect a specific molecule or a family of molecules. In addition, continuous efforts have been produced towards the development of new methods to increase the sensitivity of the pSi biosensors.[20] In particular, organic/inorganic hybrid systems combining the intriguing chemical properties of the organic part with the optical and morphological features of the inorganic pSi substrate allow to improve the selectivity and sensitivity of the sensing devices.[9,11,13,21–23] More recently responsive polymer hydrogels have been incorporated into pSi matrices, highlighting the promising use of such hybrid smart polymer/transducer systems in areas including drug delivery, biosensing and implants.[24–27] Particular interest currently concerns the detection of specific class of drugs such as nonsteroidal anti-inflammatory (NSAI) (ibuprofen, naproxen and diclofenac), that are regularly used by patients, often without medical prescription, and that are potentially harmful when present in water-like environment.[1] NSAI drug molecules are simple small carboxylic acid-containing molecules, with negative charge at neutral pH in aqueous environment. Carboxylic acid-containing molecules display high affinity toward amine-containing molecules undergoing complexation reaction. Chitosan is a polycationic, biodegradable natural polymer of β-(1,4)-linked D-glucosamine obtained by alkaline deacetylation of chitin. Under certain conditions, chitosan has an important surface charge distributed on the entire chain that can be adjusted by simply varying the solution pH.[28,29] The pH sensitivity of chitosan arises from the large number of amino groups present on the polymer, and is very interesting for biosensing purposes. Combining pH sensitive chitosan polymer with porous silicon substrate had revealed very interesting properties for drug delivery applications.[30,31] Here we describe

[a]*Institut Charles Gerhardt Montpellier, UMR 5253 CNRS-ENSCM-UM2-UM1, Matériaux Avancés pour la Catalyse et la Santé, Ecole Nationale Supérieure de Chimie de Montpellier, 8 rue de l'Ecole Normale, 34296 Montpellier, France. E-mail: frederique.cunin@enscm.fr; Fax: (+33)467163470; Tel: (+33)467163444*
[b]*Dipartimento di Scienza dei Materiali ed Ingegneria Chimica, Politecnico di Torino, C.so Duca degli Abruzzi 24, 10129 Turin, Italy*

the preparation, characterization and sensing properties of a new chitosan/porous silicon hybrid biosensing platform, where oligomers of chitosan are covalently attached to porous silicon films, for the detection of carboxylic acid-containing molecules in water.

Experimental

Preparation of the porous silicon films

Porous silicon layer was fabricated by electrochemical etch of highly boron-doped monocrystalline (100) silicon substrate (p-type, 0.9523 mΩ cm) (Siltronix, Inc), with a current density of 75 mA cm^{-2} for 180 s in a solution of HF (48%, SIGMA Aldrich), ethanol (99.98%, SIGMA Aldrich) in a 3 : 1 volume ratio; after the etch, the sample was thoroughly rinsed with ethanol (three times) to remove any HF trace and dried under a stream of nitrogen. Previously to the etch, the silicon wafer underwent a two-step chemical pre-treatment in order to inhibit the formation of a parasitic surface layer during the etch.[32] In the first step, the wafer was heated in air at 400 °C for 2 h, then exposed to a HF, H$_2$O, ethanol (1 : 1 : 3 volume ratio) solution for 5 min in order to remove the oxide layer formed during the thermal treatment. In a second step, the clean wafer was shortly etched using a current density of 75 mA for 30 s, and exposed to a 0.1 M NaOH solution for two minutes. The chip was exposed to a HF, H$_2$O, ethanol (1 : 1 : 3 volume ratio) solution and then rinsed three times with ethanol and dried under a stream of nitrogen.

Prior to grafting the oligomers of chitosan, freshly etched porous silicon hydride-terminated surface was hydrosilylated with an excess of neat undecylenic acid (SIGMA Aldrich), under argon atmosphere at 130 °C for two hours. The pSi sample was then successively rinsed with ethanol, acetone and ethanol to wash away any undecylenic acid physisorbed on the surface, and dried under a stream of nitrogen.

Preparation of the chitosan oligomers

Chitosan oligomers of controlled molecular weight (1.6 × 10^4 g mol^{-1}, polydispersity: 1.3 ± 0.3) were prepared by depolymerisation of chitosan (degree of acetylation = 0.1, average molecular weight = 7 × 10^5 g mol^{-1}, Sigma Aldrich). Depolymerization of chitosan in oligomers of controlled molecular weight was achieved by hydrolysis of the polymer with controlled amount of sodium nitrate.[33] In a typical preparation, 650 mg of chitosan were dissolved in 30 ml of aqueous acetic acid solution (0. 88%) (w/w) (Sigma Aldrich) and stirred overnight. After complete dissolution, 443 μl of sodium nitrate (Sigma Aldrich) were added to the chitosan solution, which was stirred overnight. The solution was precipitated by adding an excess of ammonia under stirring for 45 min, and then centrifuged for 15 min. The compound was then rinsed with deionized water and dried by lyophilization. The molecular weight of the obtained compound was measured by size exclusion chromatography (SEC) coupled online with a multi-angle laser light scattering (MALLS) detector. SEC was performed by means of a Shimadzu LC-GA pump connected to Shodex OHPak SB-LG and OHPak SB-805HQ columns. A shimadzu RID 6A refractometer and a multi-angle laser-light detector (Wyatt Dawn DSP) were connected online.

Grafting of the chitosan oligomers onto the porous silicon films

6 mg of the as-prepared chitosan oligomers (1.6 × 10^4 g mol^{-1}) were dissolved in a 0.16% acetic acid solution (3 ml), and stirred overnight. The pH of the chitosan solution was adjusted to 7 by adding 0.1 M NaOH (Sigma Aldrich). Crosslinking of the carboxylic acid functions present at the surface of porous silicon with the amine groups of chitosan was performed in a two-step reaction.[34] The coupling solution (12 mg of EDC (1-ethyl-3-(3-dimethylaminopropyl)-carbodiimide, Sigma Aldrich) and 12 mg of NHS (N-hydroxysuccinimide, Sigma Aldrich) in 3ml of Milli-Q water, with pH adjusted to 6) was first reacted with pSi sample for 30 min at room temperature; then pSi was rinsed with deionized water and dried under a stream of nitrogen. The pSi sample was then exposed to the solution of chitosan oligomers overnight to insure deep penetration of the polysaccharide inside the porous matrix of silicon. After reaction, the pSi sample was successively rinsed in a 0.16% aqueous acetic acid solution and in several ethanolic solutions with an increasing content of ethanol, ranging from 10% to 100%. Supercritical CO$_2$ drying (slightly beyond 73 bar and 31 °C in a Polaron 3100 apparatus) was carried out to avoid chitosan shrinkage during drying step.[35,36]

Preparation of the drug solutions

A master solution of 0.1 mg ml^{-1} of ibuprofen was prepared by dissolving pure ibuprofen (Sigma Aldrich) in Milli-Q water. 0.8% of absolute ethanol (Sigma, Aldrich) was added to the solution in order to increase the solubility of ibuprofen in water. Lower concentrated ibuprofen solutions were obtained by dilution of the master solution. The pH of the solutions was adjusted to the desired value by adding HCl.

A 0.05 mg ml^{-1} solution of caffeine was prepared by dissolving pure caffeine (Sigma Aldrich) in Milli-Q water. 0.8% of absolute ethanol (Sigma, Aldrich) was added to the solution in order to increase the solubility of caffeine in water. The pH of the solutions was adjusted to the desired value by adding HCl.

A 1 mg ml^{-1} solution of β-hydroxybutyric acid was prepared by dissolving pure β-hydroxybutyric (Sigma Aldrich) in Milli-Q water. 0.8% of absolute ethanol (Sigma, Aldrich) was added to the solution in order to increase the solubility of β-hydroxybutyric acid in water. The pH of the solutions was adjusted to the desired value by adding HCl.

Characterization of the porous silicon films

Scanning electron microscopy (SEM) images were obtained using a high resolution Field Emission Gun S-4800 Hitachi microscope operating at 30 kV. To avoid sample charging anomalies, the porous Si samples were metalized with a thin layer of gold prior to the SEM analysis.

Nitrogen adsorption–desorption isotherms of the pSi films were recorded at 77 K using a Micromeritics ASAP 2020 volumetric apparatus. Prior to the adsorption experiment, the samples were outgassed overnight in situ at 298 K. The surface area of the sample was measured by the BET

(Brunauer–Emmett–Teller) method, which yields the amount of adsorbate corresponding to a molecular monolayer.[37,38] The specific surface area of the porous matrix and the porous volume were expressed per geometrical unit area of pSi sample. The pore dimensions were determined by using the BdB (Broekhof–de Boer) method from the nitrogen adsorption curve.[39] Even though the adsorption curve is less often used than the desorption curve for pore size determination, it presents the significant advantage of being independent of pore constrictions.[40] The mesoporous volume was measured as the adsorbed volume at the top of the capillary condensation step of the isotherm.

PSi films were characterized by FTIR spectroscopy, in attenuated total reflectance mode with a Bruker Tensor 27 spectrometer equipped with an ATR (Attenuated Total Reflectance) collector system.

The optical measurements were carried out by specular reflectance spectroscopy in the range 200–3200 nm with a Varian Cary UV5000 equipped with a reflectance cell at 12°.

Interferometric reflectance spectra measurements

The reflectance spectra of porous silicon films were recorded using an Ocean Optics CCDS-2000 spectrometer coupled to a bifurcated optical fiber, in the range 400–1000 nm, in a back-reflection configuration. A tungsten light source was focused onto the center of the porous silicon surface, and the reflected light was detected back along a direction normal to the surface sample. According to a method referred to as Reflective Interferometric Fourier Transform Spectroscopy (RIFTS),[13,41] a fast Fourier transform (FFT) was applied to the reflectance spectrum (algorithm from the Wavemetrics Inc. (www.wavemetrics.com) IGOR program library (FFT)).

Flow cell experiments

Drug sensing experiments were carried out in a plexiglass homemade flow cell, connected *via* an outlet to a peristaltic pump working in a pulling mode. The light beam was focused onto the porous silicon surface through a plexiglass transparent window and reflectance spectra were recorded.

Calculations of the percentages of the protonated species in water at various pH were performed using the following relationship: $\mathrm{pH} = \mathrm{p}K_a + \log[\mathrm{A}^-]/[\mathrm{AH}]$ (1)

Results and discussion

Characterization of the porous silicon matrix

The porosity and thickness of the freshly etched porous silicon films were characterized by scanning electron microscopy (SEM) and optical measurements.

Samples were electrochemically etched at a current density of 75 mA cm^{-2} for 180 s in a 3 : 1 (v/v) HF : ethanol solution. Previously to the etch, the silicon wafer was pre-treated in a two-step process in order to prevent the formation of a parasitic layer at the top surface of the porous film. Indeed, the presence of a parasitic layer which exhibits obstructed porosity at the top surface of the pSi film (Fig. 1a) is highly undesirable for the incorporation and diffusion of large molecules within the porous matrix; its presence also has been shown to affect the optical

quality of the porous silicon film.[42] The formation of a parasitic layer of few tens of nanometres has been described earlier in the literature particularly for pSi samples etched from highly doped *p* type silicon.[32,43] Chamard *et al.* ascribed the origin of the
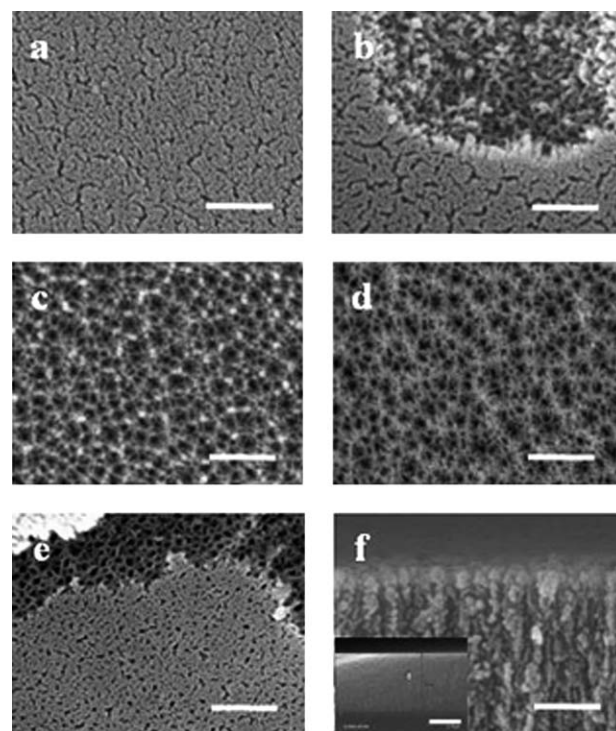

Fig. 1 SEM images of freshly etched porous silicon matrices. Scale bars are 300 μm. The samples were etched using the same following conditions: 75 mA cm^{-2} for 180 s in a 48% aqueous HF : ethanol (3 : 1) (v/v) solution. Various pre-treatments of the precursor silicon wafer were realized prior to the etch: (a) no pre-treatment was performed on the silicon wafer prior to the etch. (b) A thermal pre-treatment was realized on the silicon wafer prior to the etch using the following conditions: the wafer was heated in air at 400 °C for 2 h, then exposed to a HF, H$_2$O, ethanol (1 : 1 : 3 volume ratio) solution for 5 min in order to remove the oxide layer formed during the thermal treatment, and rinsed three times with ethanol. (c) A two-step pre-treatment was realized on the silicon wafer prior to the etch according to the following conditions: the wafer was heated in air at 400 °C for 2 h, then exposed to a HF, H$_2$O, ethanol (1 : 1 : 3 volume ratio) solution for 5 min. The wafer was then shortly etched using a current density of 75 mA for 30 s in a 48% aqueous HF : ethanol (3 : 1) solution, and exposed to a NaOH solution (0.1 M) for two minutes in order to dissolve the as-formed porous film. The chip was exposed to a HF, H$_2$O, ethanol (1 : 1 : 3 volume ratio) solution and then rinsed three time with ethanol and dried under a stream of nitrogen. (d) The silicon wafer was shortly etched at 75 mA for 30 s in a 48% aqueous HF : ethanol (3 : 1) solution, and exposed to a NaOH solution (1 M) for two minutes. The chip was exposed to a HF, H$_2$O, Ethanol (1 : 1 : 3 in volume) solution and then rinsed three time with ethanol and dried under a stream of nitrogen. (e) The silicon wafer was etched at 75 mA for 180 s in a 48% aqueous HF : ethanol (3 : 1) solution, then electropolishing current of 4 mA cm^{-2} was applied for 240 s in a 3 : 1 (v/v) HF : ethanol solution in order to remove the as-formed porous layer, and the wafer was etched again at 75 mA for 180 s in a 48% aqueous HF : ethanol (3 : 1) solution. (f) Cross-sectional SEM image. The silicon wafer was pre-treated according to the procedure described in (c). Offset shows a larger view of the cross-section with a thickness of the porous layer of 7.44 μm. Scale bar in the offset is 3.75 μm.

parasitic layer to a contamination of the top layer of the silicon substrate by hydrogen atoms incorporated during the silicon wafer manufacture.[32] Passivation by hydrogen of the boron doping atoms used in p type silicon locally changes the resistivity of the silicon wafer consequently leading to the generation of a porous layer not homogenous in depth.

Several approaches including chemical cleaning, thermal treatment, electropolishing, chemical etching and plasma etching have been proposed to inhibit the formation of the parasitic layer[32,44] or remove it after formation.[43] Errien *et al.* proposed a simple efficient method which consists in chemical dissolution in NaOH of the porous parasitic layer once it's formed, but such a treatment modifies the morphology and the surface chemistry of the pSi samples.[46] Plasma etching allows to remove the parasitic layer with a very good reproducibility compared to the chemical dissolution with NaOH, without modifying the morphology and surface chemistry of the pSi films, but it requires more sophisticated experimental set-up. Ultrasonication allows removal of the parasitic layer but also breaks the porous structures. Chamard *et al.* reported a thermal pre-treatment of the wafer, followed by chemical dissolution of the formed oxide layer at the top surface of the wafer as a successful method to prevent the formation of a parasitic layer.[32]

In the present work, we first tried this latest method of thermal pre-treatment proposed by Chamard on the silicon wafer, prior to etch. Surface SEM image of the resulting porous film is presented in Fig. 1b. It revealed a slightly more opened porosity compared to the SEM image in Fig. 1a where no pre-treatment of the wafer was processed previously to the etch, but a nonhomogeneous porosity in depth was also observed with the presence of a second opened porous layer underneath the top one. This observation led us to the development of a two-step pre-treatment method, which firstly consists of a thermal treatment of the wafer with removal of the formed oxide layer in a HF/ethanol solution, and secondly consists of a short electrochemical etching followed by removal of the porous layer in a sodium hydroxide solution. SEM image of a porous film etched from a wafer pretreated with the two-step method is presented in Fig. 1c. Single opened porosity with pore size of 10 to 50 nm was successfully produced.

Note that we also observed that the "second step" including short electrochemical etching followed by exposition to NaOH solution is efficient itself as a single step treatment and the thermal treatment first step is not indispensable to avoid the formation of the parasitic layer (Fig. 1d). But all the samples in this work have been prepared with the two-step pre-treatment prior to etch. We also tried to remove the porous layers of silicon by electropolishing instead of by dissolution in sodium hydroxide prior to the etch, but it did not prevent the formation of a parasitic layer (Fig. 1e). Possible incorporation of H atoms into silicon during porous silicon formation, demonstrated by Levy-Clément[47] could explain this result. In this case, H atoms diffuse at the pSi/Si interface and inside the silicon crystallite in the pore walls during anodization. Thus H atoms could contaminate the bulk Si underneath the pores tips and passivate the boron atoms, which was proposed as a possible cause for parasitic layer formation. Classical [100]-orientated pores were observed with homogeneous diameter at the pore mouth and in depth. Thickness of the films was measured at 7.44 μm (Fig. 1f).

The optical reflectivity spectrum displays fringes which result from Fabry–Pérot interferences at the two boundaries of the porous silicon layer. The position of the fringes maxima is given by the following relationship:

$$m\lambda = 2nL \tag{2}$$

where m is the spectral order, n is the refractive index of the film, L is the thickness of the film, and λ is the wavelength of the incident light for maximum constructive interferences. The product nL corresponds to the optical thickness of the film. Its value can be extracted directly from the reflectance spectrum by applying a fast Fourier transform (FFT).[13,41] A best-fit calculation of the reflectance spectrum was performed using a commercial code SCOUT.[45] The method has proved reliable for the determination of the physical parameters (porosity and thickness) of pSi films, when applied on a large spectral window of the reflectivity spectrum.[42] Using an optical method for the determination of the porosity has the advantage of being nondestructive compared to a gravimetric method, where cumulative errors on multiple mass measurements are also probable. In this approach the refractive index of the pSi film (n_{pSi}) was calculated applying a Bruggeman approximation[46,48] for each wavelength according to the following relationship:

$$(1 - P)\frac{n_{si}^2 - n_{pSi}^2}{n_{si}^2 + 2n_{pSi}^2} + P\frac{n_{void}^2 - n_{pSi}^2}{n_{void}^2 + 2n_{pSi}^2} = 0 \tag{3}$$

where P is the porosity, n_{si} the refractive index of the silicon substrate and n_{void} the refractive index of the filling material (air for instance). The values of the porosity and thickness, which are the two free parameters of the model in the SCOUT simulation, were adjusted in order to get the best fit between the experimental and the theoretical spectra. Typically, at each wavelength, reflectance of the layer stack is calculated and compared to the experimental one by adjusting porosity and thickness of the sample, and a best fit over the whole wavelength range is obtained. It resulted in a calculated porosity of 71% and a calculated thickness of 7.4 μm for the freshly etched porous silicon film. The calculated thickness of the porous layer obtained in such a way is in perfect agreement with the SEM measurements.

Chemical modification and characterization

Freshly etched porous silicon hydride-terminated surface was first hydrosilylated with undecylenic acid in order to provide the pSi surface with carboxylic acid terminus functions. The carboxylic acid functions present at the surface of porous silicon were crosslinked with the amine groups of the chitosan oligomers by carbodiimide coupling chemistry using EDC and NHS coupling agents. An aqueous solution of EDC and NHS was first reacted with the carboxylic acid terminated pSi surface; this step created a semi-stable amine-reactive ester suitable for further reaction with the primary amines present on the chitosan oligomers chains. After successive rinsing cycles, supercritical CO_2 drying was performed in order to avoid chitosan shrinkage during drying step which was observed to result in the pSi structure collapse when dried by solvent evaporation (Fig. 2a). The samples were characterized by Fourier-transform infrared

This journal is © The Royal Society of Chemistry 2011

J. Mater. Chem., 2011, **21**, 2294–2302 | 2297

(FTIR) spectroscopy (Fig. 2b) and SEM (Fig. 2c and d) at every functionalization step.

Fig. 2b shows the FTIR spectra in attenuated total reflectance (ATR) mode for (A) a pSi surface functionalized with undecylenic acid, and (B) the previously undecanoic acid-functionalized pSi surface after reaction with the chitosan oligomers. After hydrosilylation of the pSi surface with undecylenic acid, spectrum (A) exhibits a band at 1710 cm^{-1}, assigned to the $\nu_{C=O}$ stretching vibration mode of the carboxylic acid, and bands at 1463, 2926 and 2854 cm^{-1} that are assigned to the deformation and stretching (symmetric and asymmetric) vibration modes of the aliphatic C–H$_2$ groups respectively. The presence of bands at 630, 905 and 2100 cm^{-1}, respectively assigned to the Si–H rocking mode, Si–H$_2$ bending mode and to the Si–H$_x$ stretching mode indicates that part of the silicon hydride remains unreacted at the pSi surface.[49] In addition the band at 1060 cm^{-1} assigned to the Si–O stretching vibration mode attests the presence of silicon oxide at the surface of pSi that forms during thermal hydrosilylation even if the reaction was performed under inert atmosphere.

After the crosslinking reaction with the amine groups of the chitosan oligomers in the presence of EDC and NHS, bands were observed in spectrum (B) at 1650 and 1543 cm^{-1} corresponding to the amide I and amide II bands respectively, indicating that the chitosan oligomers covalently bonded to the acid terminus on the pSi surface. The large broad band formed at 3350 cm^{-1} is associated to both the O–H stretching vibration mode from the chitosan, and the N–H stretching vibration mode from the amine functions on chitosan that remained unreacted after the crosslinking reaction, as well as N–H stretching vibration mode from the secondary amides. The strong band at 1040 cm^{-1} is assigned to the Si–O stretching vibration mode, although the contribution of the C–O stretching in the chitosan, which appears in the same region, cannot be excluded. The presence of $\nu_{C=O}$ stretching vibration mode at 1710 cm^{-1} indicates that part of the carboxylic acid functions remained unreacted after the crosslinking reaction with chitosan. Finally bands were observed at 1463, 2854 and 2926 cm^{-1} due to the CH$_{tet}$ vibration mode (deformation and stretching respectively). FTIR data confirm that part of the amine functions of the chitosan oligomers have covalently attached to the undecanoic acid terminated pSi surface.

Fig. 2c and 2d show SEM surface images of an undecylenic acid, and of a chitosan functionalized pSi surfaces respectively. Pore size ranges from 15 nm to 45 nm in both cases and no obvious difference in pore size is observed by SEM after grafting chitosan oligomers into the undecylenic acid-functionalized porous silicon matrix. In addition cross-sectional SEM images of an undecylenic acid, and of a chitosan functionalized pSi film indicate that the thickness of the film remains constant after grafting the chitosan oligomers (data not shown).

In order to complete the textural characterization of the pSi matrices, measurements of nitrogen adsorption isotherms and application of the BET (Brunauer–Emmett–Teller) and BdB (Broekhof–de Boer) methods[37–40] were performed before and after grafting the chitosan oligomers. Textural and morphological characteristics determined from the N$_2$ adsorption–desorption experiments are presented in Table 1. The average pore diameter is measured at 24 nm for the undecanoic acid-functionalized pSi sample. This average value is in agreement with the values of pore diameter estimated from the SEM surface images. After grafting the chitosan oligomers, the average pore diameter is observed to decrease to 21.6 nm. The difference in the pore diameter of 2 to 3 nm is explained by the presence of chitosan species on the internal surface of the porous structure and confirms that chitosan oligomers infiltrate the pores. Indeed pores of 24 nm average in diameter (ranging from about 10 to 50 nm) are large enough to incorporate chitosan oligomers of 1.6×10^4 g mol^{-1}, considering that expected size for chitosan species in a ball conformation (which is the conformation that would display the highest steric hindrance) in appropriate conditions of solvent would be closed to 15–20 nm.[50] Surface area determined from the nitrogen adsorption measurements is significantly increased after grafting the chitosan oligomers onto the pSi surface. This increase of specific surface is certainly due to the formation of an interparticulate porosity or rugosity between the chitosan species attached at the pSi surface. Chitosan itself can display micro-structuration that is controlled by the preparation conditions. Indeed, supercritical drying performed in appropriate conditions of pressure allows the formation of aerogel forms of chitosan. Although less favorable with oligomers than with polymers[36] the formation of an aerogel form of chitosan offering additional adsorptive properties at the pSi surface cannot be excluded to explain the surface area increase after grafting chitosan. Finally the little increase in porous volume, observed after grafting chitosan is attributed to the presence of chitosan species grafted at the external surface of the pSi films. In this work, surface area and porous volume are presented per geometrical unit area of the sample and not per gram of samples as it is classically reported in the literature because surface chemistry renders dissolution process difficult for gravimetric measurements and mass sample determination.
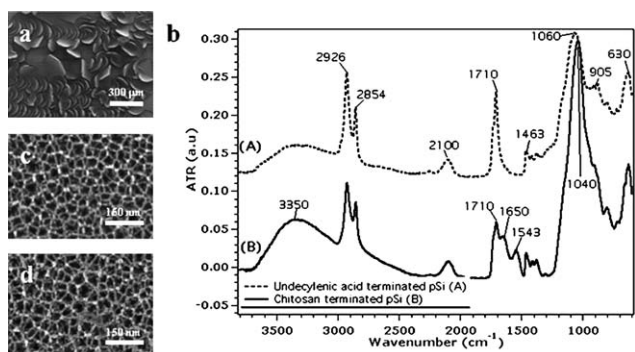

Fig. 2 (a) Surface SEM of a pSi surface after functionalization with chitosan oligomers and dried in air. Sample structure collapses due to chitosan shrinkage during drying step. (b) FTIR data for (A) an undecanoic acid-terminated pSi surface sample, and (B) the same pSi surface sample after attachment of chitosan oligomers. (c) SEM surface image of an undecylenic acid-functionalized pSi sample, (d) SEM surface image of the same pSi surface sample after attachment of chitosan oligomers.

Drug molecules sensing

The hybrid chitosan/porous silicon film was tested as an optical sensor to detect the presence of carboxylic acid-containing drug molecules in water. Drug sensing experiments were carried out in a flow cell. The reflectance spectrum of the hybrid chitosan/porous

Table 1 Textural characteristics of undecylenic acid-functionalized pSi films and of undecylenic acid + chitosan-functionalized pSi films obtained by nitrogen adsorption measurements. The porous volume and the surface area are expressed per geometrical unit area of porous silicon sample. The thickness of the porous silicon films is identical in all the samples

Surface chemistry	Average pore diameter/nm	Surface area/m² cm⁻²	Porous volume/cm³ cm⁻²
Undecylenic acid	24	0.085	0.32×10^{-3}
Undecylenic acid + chitosan	21.6	0.136	0.36×10^{-3}

Fig. 3 Variation of the optical thickness of (A) a chitosan/pSi surface and (B) an undecanoic acid terminated pSi surface, upon exposure to ibuprofen solutions of various concentrations in water with pH adjusted to 4.1. Water with pH adjusted to 4.1 is flowed between two concentration cycles as well. (C) Chemical structure of ibuprofen.

silicon film, exposed to a flow of drug solution in water, was recorded over time. A fast Fourier transform of the obtained reflectance spectrum was performed allowing direct determination of the optical thickness of the film over time as previously described in the manuscript. The principle of detection was based on the observation of changes in the optical thickness of the porous film as earlier described in the literature.[13,25] Briefly, according to relationship 2, changes in the optical thickness (nL) indicate either changes in the average refractive index of the hybrid porous film, or changes in the thickness of the film, upon introduction of analytes such as drugs within the pores. Ibuprofen was chosen as a drug model for the sensing experiments in water. Ibuprofen is a simple carboxylic acid-containing molecule of the nonsteroidal anti-inflammatory drug family which is extensively used in the treatment of rheumatic disorders, arthritis, pain and fever.[51] Ibuprofen has a pK_a of 4.5 at 25 °C and an index of refraction estimated at 1.566.[52,53]

The chitosan/porous silicon film was exposed to acidic solutions of ibuprofen in deionized water of various concentrations. Optical interferometry measurements were performed on the chitosan/porous silicon chip exposed to the ibuprofen solutions. The same experiment was performed on an undecanoic acid terminated pSi surface as a control. The undecanoic acid terminated pSi film was generated by hydrosilylation of freshly porous silicon film with undecenoic acid exactly like the hydrosilylation step described before the grafting of the chitosan oligomers. The undecanoic acid terminated pSi surface has the advantage of being chemically stable in water, and hydrophilic enough to allow diffusion of aqueous solutions within the pores. Fig. 3A reports the variations of the optical thickness over time for the chitosan terminated surface during the flowing of low concentrated solutions of ibuprofen at pH 4.1. Concentrations of the flowed solutions were successively 0.1, 1, and 10 mg l⁻¹; water with pH adjusted to 4.1 was flowed between each concentration cycle. Under these experimental conditions, the lowest detectable concentration is observed to be 1 mg l⁻¹, while no signal is detected still at 10 mg l⁻¹ for the undecanoic acid terminated surface (Fig. 3B). These results show that the sensitivity of the system increases of at least one order of magnitude when chitosan is present inside the porous matrix. The refractive index of ibuprofen is 1.566, but no significant difference was found between the refractive index of water (with pH adjusted to 4.1) and the refractive index of the solution of 10 mg l⁻¹ of Ibuprofen in water (with pH adjusted to 4.1), when measured with
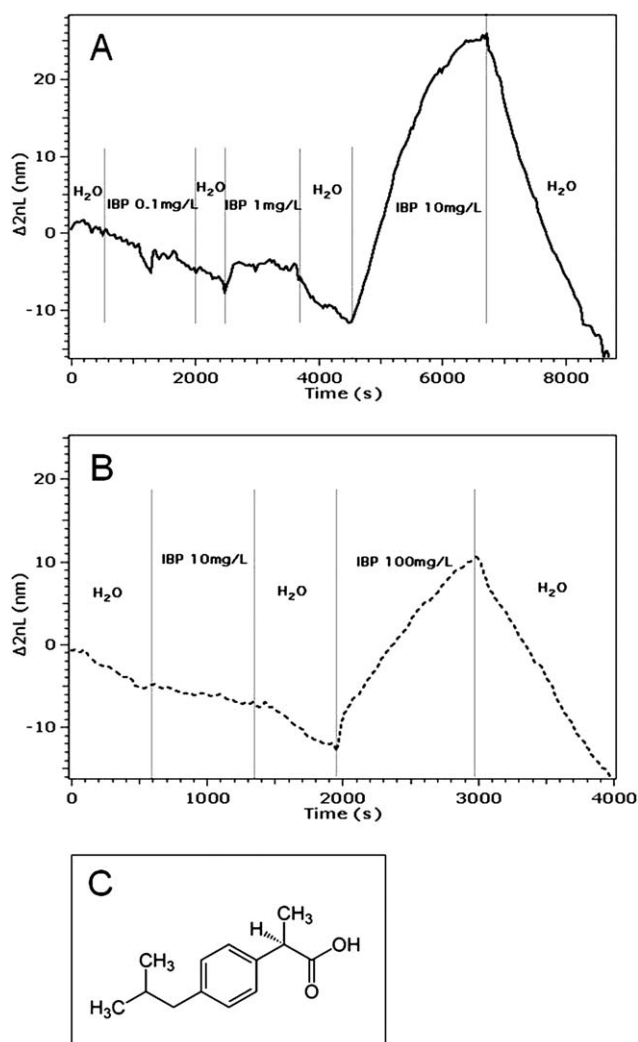
a refractometer, which highlights the role played by chitosan in the detection of ibuprofen. At pH 4.1 100% of the amino groups present on chitosan are expected to be protonated and then positively charged (pK_a of chitosan = 6.5), while 30% of the ibuprofen molecules are negatively charged (cf. eqn (1)). Solvated charged chitosan first swells into the pores of porous silicon which leads to a little increase in the optical thickness of porous silicon (Fig. 4). Then solvated charged chitosan complexes the deprotonated carboxylic acid of ibuprofen present in the solution until all the protonated amine function are neutralized, which may also lead to increasing swell of chitosan. Concentrate this way the deprotonated ibuprofen molecules inside the pores by means of a strong charge effect from swollen chitosan leads to a significant increase in the optical thickness of the pSi film and allows a strong increase of the sensitivity of the hybrid system. In comparison, shift in the optical thickness observed for the control undecanoic acid surface is attributed to the diffusion inside the pores of the 70% of the neutral ibuprofen molecules at
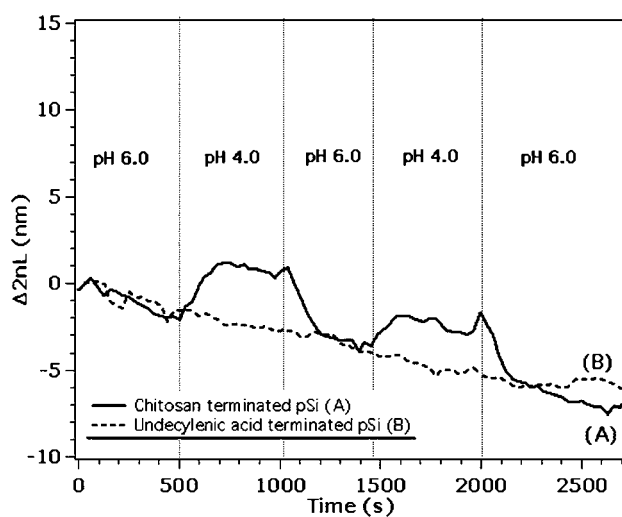
Fig. 4 Variation in the optical thickness of (A) a chitosan/pSi surface and (B) an undecanoic acid terminated pSi surface, upon flowing water at pH 6 and pH 4. Two cycles alternating the two pH are presented.

pH 4.1. For information, when pH of the solutions is switched to 6, no significant shift is observed on the control undecanoic acid terminated surface since 97% of the carboxylic acids from the surface and from ibuprofen are negatively charged, repelling each other. At pH 6 very small shift of less than 1 nm in the optical thickness is detected on the chitosan/pSi surface (data at pH 6 not shown). Finally, in order to confirm the charge effect in the detection of ibuprofen with the chitosan/pSi system, a control experiment were performed where the chitosan/pSi film and the undecanoic acid terminated control surface were exposed to a solution of 50 mg l^{-1} of caffeine at various pH. Caffeine is uncharged at the pH used in the experiments. Fig. 5 shows the variations of the optical thickness over time for (A) the chitosan terminated surface and (B) the undecanoic acid terminated surface during the flowing of a caffeine solution in water at successively pH 6, pH 5 and pH 4. No significant difference between the two surfaces in term of optical thickness variation and pH dependence was observed, except for the small 2 nm shift in water when switching pH from 6 to 5 and when switching from 5 to 4 observed only on the chitosan terminated surface. This little shift has been described earlier in the manuscript (Fig. 4A) and is attributed to swelling of chitosan when getting protonated in water. In the absence of charge on the caffeine, simple diffusion explains the shift in optical thickness observed when the porous surfaces are exposed to caffeine. Changes in the charge on chitosan do not affect the caffeine diffusion which confirms that detection of ibuprofen is based on a charge effect.

The observed change in optical thickness when binding ibuprofen to chitosan functionalized pSi surface only required few minutes to reach a steady state due to rapid diffusion into the pores of this small molecule, compared to a protein of larger size,[10] and due to strong electrostatic interactions with the surface. Typically 3 minutes were required for a corresponding shift of 4 nm for a 1 mg l^{-1} solution of ibuprofen. In comparison, releasing ibuprofen from the pores by flowing deionized water was much slower, due to the strong electrostatic interactions between the drug and the surface of the porous film at pH 4.1. In
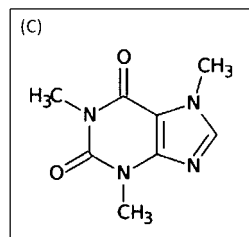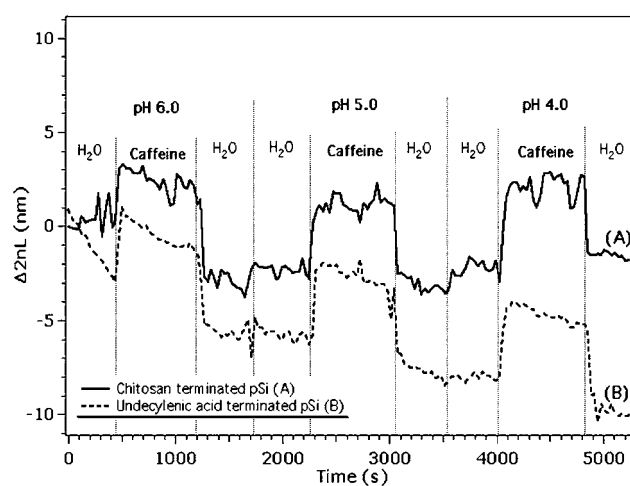

Fig. 5 Variation of the optical thickness of (A) a chitosan/pSi surface and (B) an undecanoic acid terminated pSi surface, upon exposure to a 50 mg l^{-1} solution of caffeine in water at various pH. Water with pH adjusted to the various relevant values is flowed between each pH cycle. (C) Chemical structure of caffeine.

addition the shift of the signal was governed by the amount of ibuprofen exposed to the charged surface. Rapid diffusion into the pores of the porous silicon film was also observed for caffeine, which is a small molecule too, nevertheless no difference was observed between the loading and the release profile of caffeine, presumably due to the absence of preferential interaction between the uncharged drug and the chitosan functionalized pSi surface. Finally Ibuprofen was observed to slowly release from the undecanoic acid functionalized surface, probably because of hydrogen bonding between the carboxylic acid groups from the drug and the carboxylic acid groups from the functionalized pSi surface.

In a second sensing experiment, BHB (β-hydroxybutyric acid) molecule was chosen as a possible model for GHB (γ-hydroxybutyric acid). GHB is an illegal drug also known as a date rape drug. GHB is a strong depressant of the central nervous system, it has numerous severe effects including euphoria, somnolence, nausea, respiratory difficulties, coma and death depending on the administration dose.[54] Detection of GHB is of high importance in forensic analysis and its determination in plasma and urine is usually realized by gas chromatography/mass spectroscopy methods.[55,56] In a recent publication Corma presented a colorimetric sensor array based on supramolecular host–guest complexes for the detection of GHB, definitely establishing the need of easy-to-use sensors for GHB in solution.[57] Here, we exposed a chitosan/pSi porous film to a solution of BHB. BHB is a good model for GHB since its chemical structure, molecular
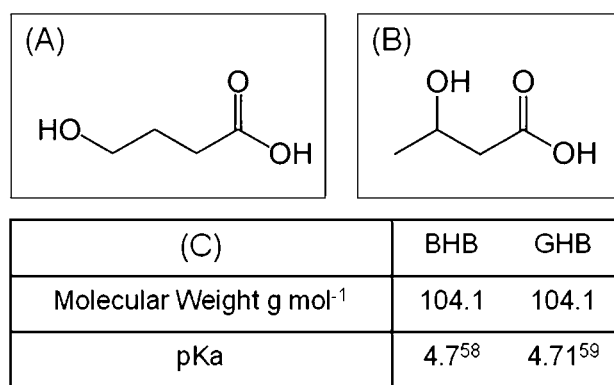
Fig. 6 Chemical structure of (A) GHB (γ-butyric acid), and (B) BHB (β-butyric acid), (C) physical and chemical properties of GHB and BHB.

weight, and pK_a are very close to GHB's (Fig. 6). Fig. 7 shows the optical thickness variations of the pSi surface functionalized with chitosan compared to the optical thickness variations of the undecanoic acid modified pSi surface when exposed to a 1 g l^{-1} acidic solution of BHB (pH 4.1). No shift in the optical thickness is detected using the undecanoic acid modified surface when the BHB solution is flowed, certainly because the index of refraction of BHB is too close to the index of refraction of water (respectively 1.444 and 1.33 (from Sigma Aldrich)) to generate a detectable difference in optical thickness at the chosen concentration. On the other hand, a rapid increase of the optical thickness is observed using the chitosan modified-surface confirming the in-pore concentration phenomena due to charge effect in the presence of solvated chitosan. In addition, in this experiment, the detected concentration at 1 g l^{-1} is right below concentrations commonly used for abuse purposes and 10 times lower than lethal concentrations,[56] considering finally that detection limit here could be further optimized to much lower concentrations.
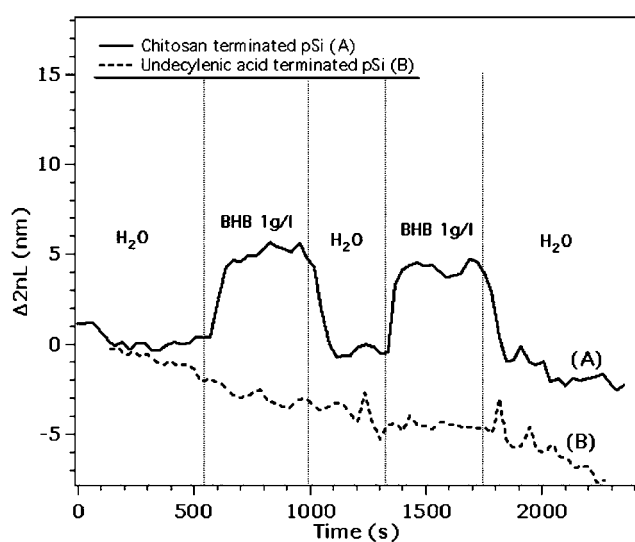

Fig. 7 Variation of the optical thickness of (A) a chitosan/pSi surface and (B) an undecanoic acid terminated pSi surface, upon exposure to a 1 g l^{-1} solution of BHB (β-butyric acid) in water with pH adjusted to 4.1. Water with pH adjusted to 4.1 is flowed between two cycles.

Conclusions

Hybrid chitosan/porous silicon films were prepared by covalent attachment of oligomers of chitosan onto the internal and external surface of porous silicon using hydrosilylation and carbodiimide coupling chemistry. The obtained hybrid films display attractive features for sensing applications: they maintain an important porosity with a higher surface area than the original pSi substrate, and offer abundant positive charges at their surface from protonated amine groups from the chitosan under appropriate pH conditions. In this work, ibuprofen was chosen as a carboxylic acid-containing drug model. Using the chitosan/pSi platform, detection of ibuprofen was demonstrated in water with a sensitivity increased by at least one order of magnitude compared to a nonfunctionalized pSi film. In addition, BHB, a model molecule for rape drug GHB was detected in water at relevant concentrations for forensic analysis with increased sensitivity using the chitosan/pSi film. The approach described here demonstrates the role that specific surface chemistry can play for improving the sensitivity of optical response in optical transducers based sensors. In addition, made of biodegradable materials, chitosan/pSi sensors are also compatible with the aqueous environment, they are easy to use, and reusable, highlighting the potential of such system for biosensing in water. Sensitivity of interest for drug pollution sensing in water is in the range of tens of nano- to micrograms per litre. 1 mg per litre of ibuprofen was detected in less than three minutes using the chitosan/pSi film, without optimization of the system. Next step concerns the optimization of the sensing properties of the porous film including sensitivity, detection time and selectivity. This effort will involve the optimization of the morphological and textural properties of the porous layer (film thickness and surface area), the optimization of the surface charge density by surface chemical modification, combined with the design of more complex optical structures such as double beam interferometer and photonic structures.[13,17]

Acknowledgements

References

1 C. C. Wong and S. L. Macleod, *J. Environ. Monit.*, 2009, **11**, 923–936.
2 McCuster, *J. Anal. Toxicol.*, 1999, **5**, 301–305.
3 K. M. Gibson, *Biol. Mass Spectrom.*, 1990, **19**, 89–93.
4 S. Guobin, S. Yan, R. D. Tyagi, R. Y. Surampalli and T. C. Zhang, *Pract. Period. Hazard., Toxic, Radioact. Waste Manage.*, 2009, **13**, 110–119.
5 N. Backmann, C. Zahnd, F. Huber, A. Bietsch, A. Pluckthun, H. P. Lang, H. J. Guntherodt, M. Hegner and C. Gerber, *Proc. Natl. Acad. Sci. U. S. A.*, 2005, **102**, 14587–14592.
6 E. Briand, M. Salmain, J. M. Herry, H. Perrot, C. Compere and C. M. Pradier, *Biosens. Bioelectron.*, 2006, **22**, 440–448.
7 L. Huang, G. Reekmans, D. Saerens, J. M. Friedt, F. Frederix, L. Francis, S. Muyldermans, A. Campitelli and C. Van Hoof, *Biosens. Bioelectron.*, 2005, **21**, 483–490.
8 M. A. Palacios, R. Nishiyabu, M. Marquez and P. Anzenbacher, Jr, *J. Am. Chem. Soc.*, 2007, **129**, 7538–7544.
9 V. S.-Y. Lin, K. Motesharei, K. S. Dancil, M. J. Sailor and M. R. Ghadiri, *Science*, 1997, **278**, 840–843.

10 K. S. Dancil, D. P. Greiner and M. J. Sailor, *J. Am. Chem. Soc.*, 1999, **12**, 7925–7930.

11 S. E. Letant and M. J. Sailor, *Adv. Mater.*, 2000, **12**(5), 355–359.

12 T. A. Schmedake, F. Cunin, J. R. Link and M. J. Sailor, *Adv. Mater.*, 2002, **14**, 1270–1272.

13 (a) C. Pacholski, M. Sartor, M. J. Sailor, F. Cunin and G. M. Miskelly, *J. Am. Chem. Soc.*, 2005, **127**, 11636–11645; (b) C. Pacholski, C. Yu, G. M. Miskelly, D. Godin and M. J. Sailor, *J. Am. Chem. Soc.*, 2006, **128**, 4250–4252.

14 M. Archer, M. Christophersen and P. M. Fauchet, *Sens. Actuators, B*, 2005, **106**(1), 347–357.

15 J. E. Lugo, M. Ocampo, A. G. Kirk, D. V. Plant and P. M. Fauchet, *J. New Mater. Electrochem. Syst.*, 2007, **10**(2), 113–116.

16 S. O. Meade, M. Y. Chen, M. J. Sailor and G. M. Miskelly, *Anal. Chem.*, 2009, **81**, 2618–2625.

17 B. Sciacca, F. Frascella, A. Venturello, P. Rivolo, E. Descrovi, F. Giorgis and F. Geobaldo, *Sens. Actuators, B*, 2009, **137**(2), 467–470.

18 E. Descrovi, F. Frascella, B. Sciacca, F. Geobaldo, L. Dominici and F. Michelotti, *Appl. Phys. Lett.*, 2007, **91**(24), 241109.

19 M. Rocchia, E. Garrone, F. Geobaldo, L. Boarino and M. J. Sailor, *Phys. Status Solidi A*, 2003, **197**(2), 365–369.

20 A. Jane, R. Dronov, A. Hodges and N. H. Voelcker, *Trends Biotechnol.*, 2009, **27**(4), 230–239.

21 C. Steinem, A. Janshoff, V. S.-Y. Lin, N. H. Voelcker and M. R. Ghadiri, *Tetrahedron*, 2004, **60**, 11259–11267.

22 N. H. Voelcker, I. Alfonso and M. R. Ghadiri, *ChemBioChem*, 2008, **9**, 1776–1786.

23 A. Tinsley-Bown, R. G. Smith, S. Hayward, M. H. Anderson, L. Koker, A. Green, R. Torrens, A. S. Wilkinson, E. A. Perkins, D. J. Squirrell, S. Nicklin, A. Hutchinson, A. J. Simons and T. I. Cox, *Phys. Status Solidi A*, 2005, **202**, 1347–1356.

24 L. A. Perelman, T. Moore, J. Singelyn, M. J. Sailor and E. Segal, *Adv. Funct. Mater.*, 2010, **20**(5), 826–833.

25 E. Segal, L. A. Perelman, F. Cunin, F. Di Renzo, J. M. Devoisselle, Y. Y. Li and M. J. Sailor, *Adv. Funct. Mater.*, 2007, **17**(7), 1153–1162.

26 L. M. Bonanno and L. A. De Louise, *Adv. Funct. Mater.*, 2010, **20**(4), 573–578.

27 L. M. Bonanno, H. Zheng, L. A. De Louise, P. M. Fauchet and B. L. Miller, *Proc. SPIE*, 2010, **7553**, 75530L, (Frontiers in Pathogen Detection).

28 J. Berger, M. Reist, J. M. Mayer, O. Felt, N. A. Peppas and R. Gurny, *Eur. J. Pharm. Biopharm.*, 2004, **57**, 19–34.

29 M. V. Risbud, A. A. Hardikar, S. V. Bhat and R. R. Bhonde, *J. Controlled Release*, 2000, **68**, 23–30.

30 J. Wu and M. J. Sailor, *Adv. Funct. Mater.*, 2009, **19**(5), 733–741.

31 P. Peng, N. H. Voelcker, S. Kumar and H. J. Griesser, *Biointerphases*, 2007, **2**(2), 95–104.

32 V. Chamard, G. Dolino and F. Muller, *J. Appl. Phys.*, 1998, **84**, 6659–6666.

33 (a) G. G. Allan and M. Peyron, *Carbohydr. Res.*, 1995, **277**, 257–272; (b) G. G. Allan and M. Peyron, *Carbohydr. Res.*, 1995, **277**, 273–282.

34 G. T. Hermanson, *Bioconjugate Techniques*, Academic Press, Inc., San Diego, 1996.

35 R. Valentin, B. Bonelli, E. Garrone, F. Di Renzo and F. Quignard, *Biomacromolecules*, 2007, **8**, 3646–3650.

36 F. Quignard, R. Valentin and F. Di Renzo, *New J. Chem.*, 2008, **32**, 1300–1310.

37 S. J. Gregg and K. S. W. Sing, *Adsorption, Surface Area and Porosity*, Academic, London, 1982.

38 S. Brunauer, P. H. Emmett and E. Teller, *J. Am. Chem. Soc.*, 1938, **60**, 309.

39 J. C. Broekhof and J. H. de Boer, *J. Catal.*, 1967, **9**, 8.

40 F. Rouquerol, J. Rouquerol and K. Sing, *Adsorption by Powders and Porous Solids*, Academic, San Diego 1999.

41 C. Pacholski, C. Yu, G. M. Miskelly, D. Godin and M. J. Sailor, *J. Am. Chem. Soc.*, 2006, **128**, 4250–4252.

42 B. Sciacca, PhD thesis, 2010.

43 N. Errien, L. Vellutini, G. Louarn and G. Froyer, *Appl. Surf. Sci.*, 2007, **253**, 7265–7271.

44 P. Allongue, C. Henry de Villeneuve, M. C. Bernard, J. E. Peou, A. Boutry-Forveille and C. Levy-Clément, *Thin Solid Films*, 1997, **297**, 1.

45 M. Theiss, Hard and Software Dr Bernhard Klein Str. 110 D-52078 Aachen, Germany, http://www.wtheiss.com/.

46 C. F. Bohren and D. R. Huffman, *Absorption and scattering of light by small particles*, Wiley, New York, 1983, p. 217.

47 P. Allongue, C. Henry de Villeneuve, M. C. Bernard, J. E. Peou, A. Boutry-Forveille and C. Levy-Clément, *Thin Solid Films*, 1997, **297**, 1.

48 E. J. Anglin, L. Cheng, W. R. Freeman and M. J. Sailor, *Adv. Drug Delivery Rev.*, 2008, **60**(11), 1266–1277.

49 R. Boukherroub, J. T. C. Wojtyk, D. M. M. Wayner and D. J. Lockwood, *J. Electrochem. Soc.*, 2002, **149**(2), H59.

50 J. Brugnerotto, J. Desbrières, G. Roberts and M. Rinaudo, *Polymer*, 2001, **42**, 9921–9927.

51 M. C. Estevez, H. Font, M. Nichkova, J. P. Salvador, B. Varela, F. Sanchez-Baeza and M. P. Marco, *The Handbook of Environmental Chemistry*, Springer Verlag, Berlin Heidelberg, 2005, 5, pp. 181–244.

52 H. Potthast, J. B. Dressman, H. E. Junginger, K. K. Midha, H. Oeser, V. P. Shah, H. Vogelpoel and D. M. Barends, *J. Pharm. Sci.*, 2005, **94**(10), 2121–2131.

53 X. Cao, B. C. Hancock, N. Leyva, J. Becker, W. Yu and V. M. Masterson, *Int. J. Pharm.*, 2009, **368**, 16–23.

54 L. Lefebvre, *Bulletin d'information toxicologique*, Institut National de Santé Publique de Québec, 1997, 13, 4.

55 G. Frison, L. Tedeschi, S. Maietti and S. D. Ferrara, *Rapid Commun. Mass Spectrom.*, 2000, **14**, 2401–2407.

56 F. J. Couper and B. K. Logan, *J. Anal. Toxicol.*, 2000, **24**, 1–7.

57 L. A. Baumes, M. B. Sogo, P. Montes-Navajas, A. Corma and H. Garcia, *Chem.–Eur. J.*, 2010, **16**, 4489–4495.

58 L. Yang, J. Zhao, P. S. Milutinovic, R. J. Brosnan and J. M. Sonner, *Anesth. Analg. (Hagerstown, MD, U. S.)*, 2007, **105**, 673–679.

59 J. V. DeFrancesco, M. R. Witkowski and L. A. Ciolino, *J. Forensic Sci.*, 2006, **51**, 321–329.